Seismic and geochemical evidence for large-scale mantle upwelling beneath the eastern Atlantic and western and central Europe

Kaj Hoernle*†, Yu-Shen Zhang‡ & David Graham§

* Earth Sciences Board and Marine Sciences Institute, ‡ Institute of Tectonics, University of California, Santa Cruz, California 95064, USA
§ College of Oceanic and Atmospheric Sciences, Oregon State University, Corvallis, Oregon 97331, USA

Seismic tomography and the isotope geochemistry of Cenozoic volcanic rocks suggest the existence of a large, sheet-like region of upwelling in the upper mantle which extends from the eastern Atlantic Ocean to central Europe and the western Mediterranean. A belt of extension and rifting in the latter two areas appears to lie above the intersection of the centre of the upwelling region with the base of the lithosphere. Lead, strontium and neodymium isotope data for all three regions converge on a restricted composition, inferred to be that of the upwelling mantle.

THE size and shape of mantle upwelling regions provide important constraints on the thermal budget of the Earth and on models of mantle dynamics. Most hotspot tracks are no more than 200–400 km wide, suggesting that upwelling regions are often relatively narrow features, of the order of a few hundred kilometres or less. But a number of geophysical observations, such as geoid and topographic anomalies and seismic tomography studies[1] indicate that at least the upper portion of upwelling regions can be significantly larger. Here we present evidence from seismic tomography, isotope geochemistry and regional geology which suggests that volcanism over a large region of the Earth's surface is related to a single, large-scale upwelling of the mantle. This region of upwelling resembles an inclined sheet and extends to depths greater than 500 km beneath the eastern Atlantic. It has a width of approximately 2,500 km in the NNE direction and bends to the east with decreasing depth for about 4,000 km beneath northern Africa, the western Mediterranean and central Europe (Fig. 1).

Regional geology

In this study, we suggest that the Eastern Atlantic volcanic province, the Western Mediterranean volcanic province and the Central European volcanic province (Fig. 1) may ultimately be derived from a common sublithospheric mantle source. The Eastern Atlantic volcanic province forms an elongate belt of islands and seamounts, which parallels the coast of northwest Africa and the Iberian peninsula. This province extends for approximately 2,500 km in the NNE direction from the Saharan seamounts and the Canary Islands in the south, to the Madeira Islands in the centre to the Biscay abyssal plain in the north. Subaerial volcanism in the Canary and Madeira islands began in the Early Miocene epoch[2,3], but submarine volcanism may have begun before 60 Myr (refs 4, 5). The western Canary and Madeira islands are situated on oceanic lithosphere, whereas the lithosphere beneath the eastern Canary Islands is transitional between oceanic and continental[6].

The Central European volcanic province extends from France to southwest Poland to Hungary and includes the Massif Central in France (where volcanism occurred between 0 and 20 Myr and between 35 and 65 Myr), the Rhenish massif (Eifel) and Rhine graben in Germany (0–20 Myr), Lower Silesia in Poland (15–40 Myr) and the western Pannonian basin in Czechoslovakia and Hungary (Eocene–Miocene and 1–12 Myr). Most of the volcanism in central Europe is related to a NNE-trending rift belt formed in the Early Cenozoic era[7]. This continental rift belt includes the Rhone, Limagne, Bresse, Rhine, Ruhr and Leine grabens. In contrast to other central European volcanism, Pannonian basin volcanism is associated with back-arc spreading[8].

The Western Mediterranean volcanic province includes the Roman province of Italy (Quaternary period), the Aeolian Islands (Quaternary), eastern Sicily (Late Cretaceous–Quaternary), the Straits of Sicily (late Miocene–Holocene) and Sardinia and Corsica (Oligocene–Pleistocene)[8]. Each of these volcanic regions is underlain by continental crust which has been undergoing extension, as evidenced by intensive block-faulting and rifting. During the late Oligocene–early Miocene, the Balearic, Valencia and Algerian rifts formed in the western Mediterranean, extending the NNE-trending rift belt in central Europe to the southwest for a total length[8] of more than 2,000 km. Subduction of the African plate occurred throughout the Tertiary period beneath much of the western Mediterranean, and continues to the present day beneath the Aeolian Islands.

Seismic tomography

Figures 1 and 2 show results from the global upper-mantle S-wave velocity model RG5.5[9,10]. A low S-wave velocity anomaly (LVA), with a width of about 2,500 km in the NNE direction and elongated about 4,000 km in the ESE direction, underlies the eastern Atlantic, northern Africa, the western Mediterranean and central Europe. The LVA in this model is a planar feature with a NNE strike and a westward dip.

Similar features are also found in other seismic models. Figure 3 shows NNE S-wave velocity cross-sections of the global model SH12/WM13[11] with the same locations as the profiles in Fig. 2*b*. Although their resolutions differ, both models are consistent with the presence of a large-scale, low-velocity anomaly extending from the eastern Atlantic to northern Africa, the western Mediterranean and central Europe. Local S-wave velocity models[12–14] show low-velocity regions at depths shallower than 200 km beneath western and central Europe and the Mediter-

† Present address: Department of Volcanology and Petrology, GEOMAR, Wischhofstrasse 1-3, 24148-Kiel, Germany.

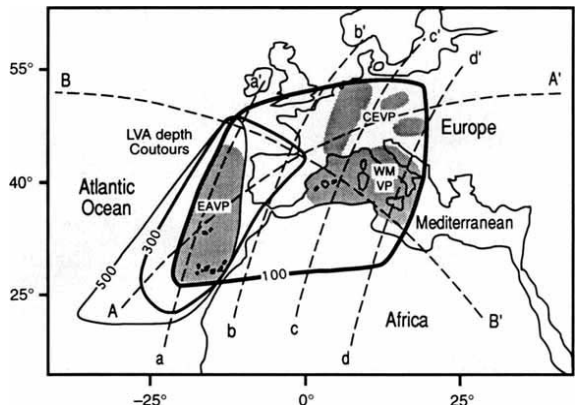

FIG. 1 Map view showing the extent of the low (less than the global mean) S-wave velocity anomaly (LVA) at depths of 100, 300 and 500 km. Where the LVA intersects the base of the lithosphere, it covers an area of 2,500 × 4,000 km, extending from the Eastern Atlantic volcanic province (EAVP) to northern Africa, the Western Mediterranean volcanic province (WMVP) and the Central European volcanic province (CEVP). The LVA becomes narrower at depth, as is indicated by the 300- and 500-km depth contours, and dips to the WNW. Volcanic provinces are denoted by shading. The locations of seismic profiles in Figs 2 and 3 are shown with appropriately labelled dashed lines.

ranean (results of local models not shown due to limited coverage of study area). Local P-wave velocity models EUR85A and EUR89A[15,16] indicate low-velocity regions at depths of 150–250 km beneath western and central Europe and the Mediterranean, whereas P-wave velocity model EUR89B[16] shows low-velocity regions between 95 and 195 km.

The correspondence in location and pattern of major anomalies for S- and P-wave tomographic models is striking, and provides evidence for a large-scale low-velocity region in the upper mantle underlying the eastern Atlantic, northern Africa, the western Mediterranean and western and central Europe. This conclusion is emphasized when we consider that many factors, such as quality and quantity of data sets, nonlinearity inversion approach, depth- and lateral-resolution differences, and dependence of velocity on temperature and volatile content, can affect inversion results for different models[16]. We interpret this low-velocity region to be a relatively hot (possibly volatile-enriched) region of mantle upwelling.

An important question concerns the detailed structure of upwelling beneath the study area. Is the LVA a single feature,

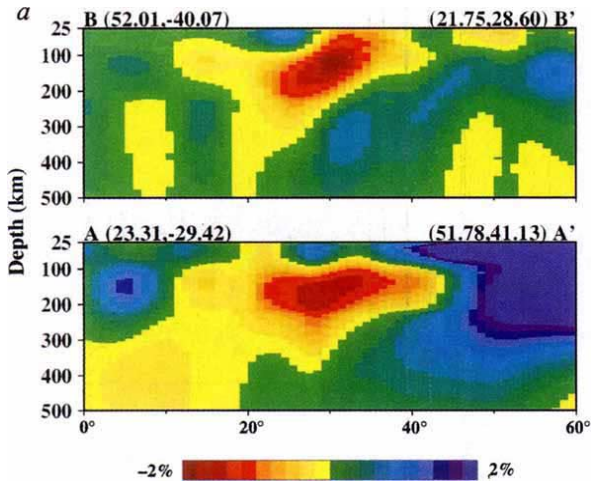

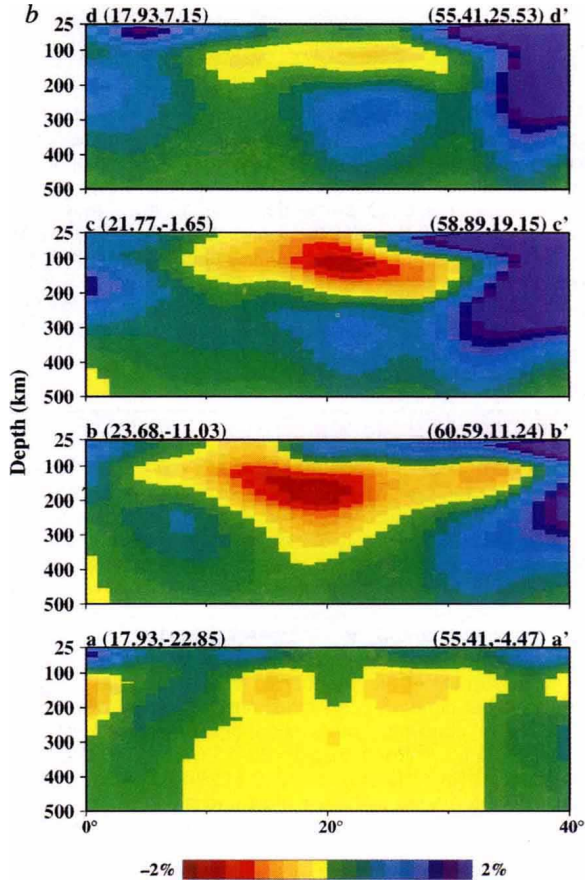

FIG. 2 Depth slices from 25 to 500 km for S-wave seismic velocity model RG5.5[9,10]: *a*, in the northeast and southeast directions; *b*, in the NNE directions (profile locations shown in Fig. 1). The sheet-like LVA strikes to the NNE and dips to the WNW. It is ~2,500 km along strike, has a maximum thickness of 500–800 km, and extends to depths >500 km beneath the Eastern Atlantic volcanic province (EAVP). The centre of the sheet encounters the base of the lithosphere some 2,000 km to the east of the EAVP beneath the central European–western Mediterranean rift system. The two smaller low-velocity maxima between 100 and 200 km depth beneath the eastern Atlantic (profiles BB′ and aa′) may result from secondary instabilities rising from the inclined sheet at 200–300 km depth. A similar concept has been proposed for inclined plume conduits, but on a smaller scale[37,48]. The fast velocity anomalies in profiles BB′ (30°–50°) and dd′ (18°–30°) may reflect stacking of subducted African oceanic lithosphere, which is being subducted with a northwest dip beneath the Aeolian Islands. Model RG5.5, obtained from surface-wave data, has a horizontal resolution of ~1,000 km and a vertical resolution of ~50 km at 50 km depth, and 300 km at 400 km depth; thus, this model cannot resolve subducted slabs thinner than 100 km. Velocity anomalies (see colour scale at bottom of panels *a* and *b*) are given in percentage of the global mean at each depth, contoured at 0.4% intervals. Endmember coordinates, at the top of each profile, are given as (latitude, longitude) in degrees of a great circle. The horizontal axis is the distance in degrees (1° ≡ 111 km) from the first latitude and longitude specified at the top of each section.

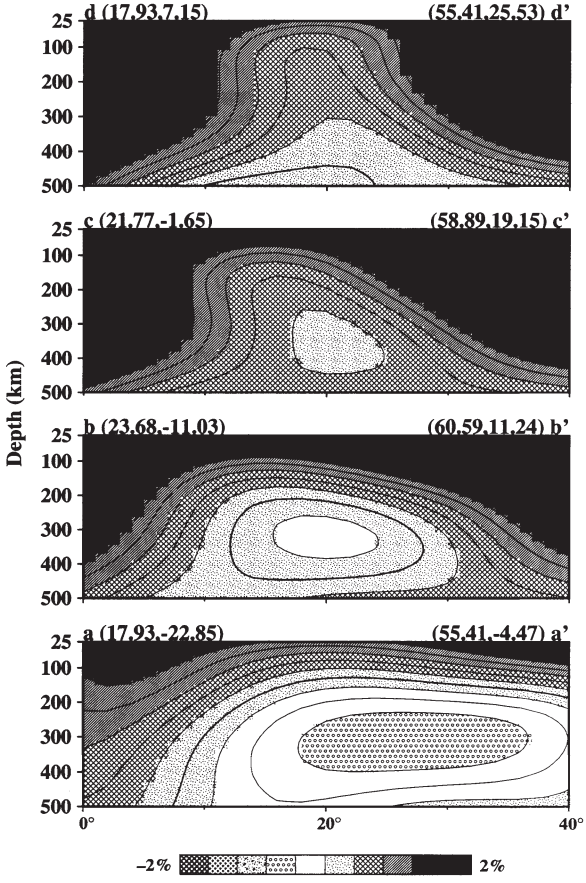

FIG. 3 North–south depth slices through the S-wave velocity anomaly in model SH12/WM13[11], which have the same locations as the depth slices in Fig. 2*b*. Model SH12/WM13 has increased resolution at greater depths (lower-mantle) than model RG5.5, but only one-third the resolution at shallower depths (upper-mantle). Nevertheless, the low-velocity anomaly in model RG5.5 in clearly seen in model SH12/WM13. Model SH12/WM13 shows the largest low-velocity anomaly at depths of 250–400 km beneath the eastern Atlantic. In contrast, model RG5.5 with its improved resolution at shallower depths shows the largest low-velocity anomaly beneath Europe and the Mediterranean. See Fig. 2 legend for additional information.

or does it reflect an averaging of spatially isolated low-velocity regions, such as a cluster of plumes which are smaller than the resolution of model RG5.5? Local P-wave model EUR89B[16] shows laterally separated anomalies beneath Europe and the western Mediterranean, although we note that models EUR85A[15] and EUR89A[16] (with only slightly different reference models) for the most part do not. Whether the laterally separated anomalies in EUR89B represent multiple small plumes, however, cannot be resolved with this model, because the depth resolution over most of the area of interest (150–400 km) is relatively poor[16]. The recent local S-wave model EUR-S91[13,14] has excellent reported lateral and depth resolution. This model shows the LVA to be continuous within the stated resolution,

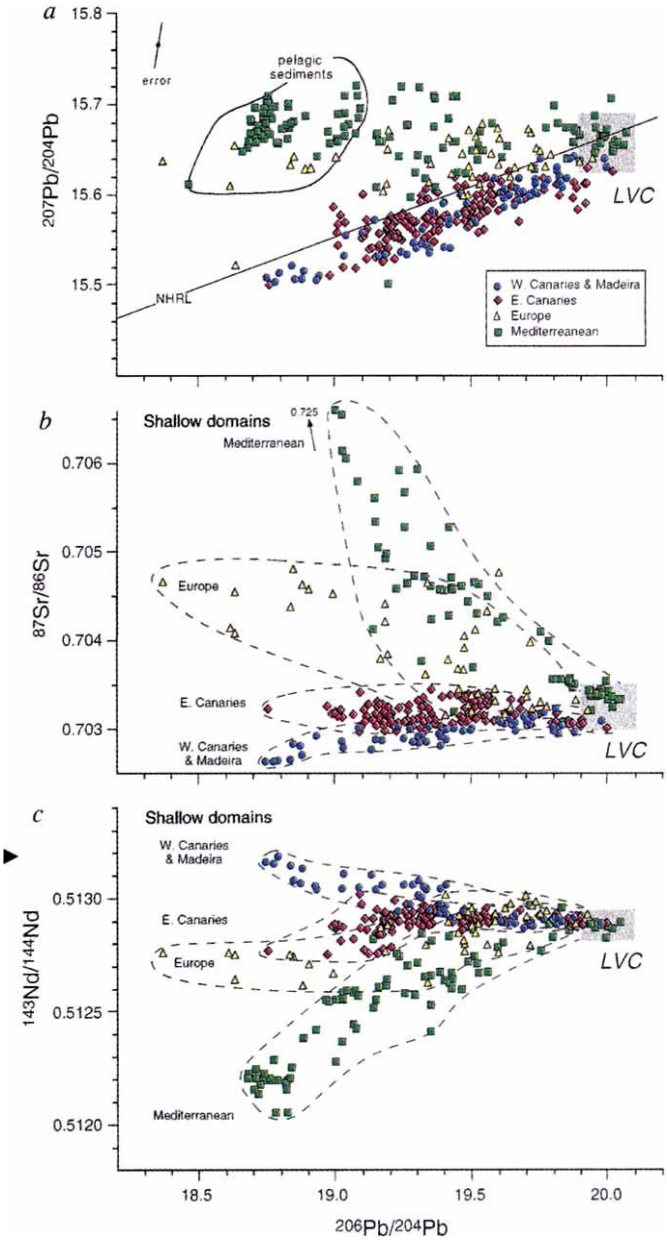

FIG. 4 Plots of $^{206}Pb/^{204}Pb$ against $^{207}Pb/^{204}Pb$ (*a*), $^{87}Sr/^{86}Sr$ (*b*) and $^{143}Nd/^{144}Nd$ (*c*) for Cenozoic volcanic rocks from four geographical regions: (1) eastern Atlantic oceanic domain, which includes the western Canary and Madeira islands (circles); (2) eastern Atlantic continental margin domain, consisting of the eastern Canary Islands (diamonds); (3) central European continental domain, including mafic volcanic rocks and carbonatites from the Massif Central, Rhenish massif, Rhine graben, Eger graben and Pannonian basin (triangles); and (4) western Mediterranean domain, containing Italy, Sicily, the Aeolian Islands and islands in the Straits of Sicily (squares). The isotope data from these four geographical domains form fan-shaped patterns. The data array for each region converges on a common composition with $^{206}Pb/^{204}Pb \cong 19.9–20.1$, $^{207}Pb/^{204}Pb \cong 15.62–15.68$, $^{87}Sr/^{86}Sr \cong 0.7030–0.7034$ and $^{143}Nd/^{144}Nd \cong 0.51282–0.51294$ ($\varepsilon_{Nd} = 3.5–5.9$). This component is interpreted as having the composition of the low-velocity anomaly shown in Figs 1–3 and is therefore referred to as the low-velocity component (LVC). For each geographical region, the component(s) with lower $^{206}Pb/^{204}Pb$ is/are located in the lithosphere or shallowest asthenosphere. Possible endmember compositions for the shallower components are indicated in *b* and *c*. These shallow regional domains may primarily reflect (1) depleted oceanic lithosphere and asthenosphere (western Canary and Madeira islands), (2) transitional oceanic/continental type lithosphere (eastern Canary Islands), (3) lower crust and/or lithospheric mantle affected by ancient subduction (central Europe), and (4) upper crust and/or lithospheric mantle and asthenosphere influenced by recent subduction (western Mediterranean). The Northern Hemisphere reference line (NHRL)[49], the field for deep-sea (pelagic) sediments[50,51] and standard error due to mass fractionation of 0.5% per atomic mass unit are shown in *a*. Standard errors for $^{87}Sr/^{86}Sr$ and $^{143}Nd/^{144}Nd$ are generally smaller than the height of the symbols. Only data from samples analysed for Sr, Nd and Pb isotopes are shown. Data sources are refs 6, 18–26, 28, 31 and 52–58.

and does not show any evidence for deep roots of the LVA beneath central Europe or the western Mediterranean, in good agreement with global model RG5.5 used here.

Nevertheless, some degree of lateral discontinuity in the LVA is to be expected. It could result from localized up- and downwellings near the lithosphere–asthenosphere interface, or rising blobs and pipes of hot and/or volatile-rich mantle surrounded by cooler asthenospheric mantle entrained at shallower depths[17]. Although detected by volcanological and petrological methods[17], such mantle structures, with diameters of less than 100 km, are beyond the resolution presently available with seismic tomography. The isotope geochemistry of Cenozoic volcanic rocks from regions overlying the LVA provides additional evidence that the LVA is a large-scale region of mantle upwelling.

Isotope geochemistry

Isotope data from Cenozoic volcanic rocks overlying the LVA are shown in Fig. 4. The data have been subdivided into four groups based on regional domain: (1) eastern Atlantic oceanic domain (western Canary and Madeira islands), erupted on oceanic lithosphere; (2) eastern Atlantic continental margin domain (eastern Canary Islands), erupted on lithosphere which is transitional in character between oceanic and continental; (3) central European domain, erupted on continental lithosphere and apparently affected to some degree by ancient subduction associated with the Hercynian orogeny[18]; and (4) western Mediterranean domain, a region influenced by recent subduction. The data for each group form trends crudely consistent with binary mixing. The arrays for each region converge on a restricted compositional range, which we interpret as being the isotope composition of the seismic low-velocity anomaly and henceforth refer to as the low-velocity composition (LVC).

The $^{206}Pb/^{204}Pb$ ratio for volcanic rocks from the eastern Atlantic oceanic domain correlates positively with $^{207}Pb/^{204}Pb$, $^{208}Pb/^{204}Pb$ (not shown) and $^{87}Sr/^{86}Sr$, and negatively with $^{143}Nd/^{144}Nd$ (Fig. 4). The $^{87}Sr/^{86}Sr$ ratio correlates negatively with $^{143}Nd/^{144}Nd$ (not shown). Lavas from the western Canary Islands have isotope compositions that overlap the LVC[6,19], whereas some lavas from Madeira have isotope compositions similar to average Atlantic normal mid-ocean-ridge basalts (N-MORBs) (ref. 20 and K.H., unpublished data). A lithospheric mantle source has been proposed for this depleted Madeira endmember[20,21], although a shallow asthenospheric origin cannot be excluded. Mixing of the LVC and shallow depleted mantle can account for the range of isotope compositions in the western Canary and Madeira islands.

The eastern Canary Islands have isotope compositions which extend from the LVC to higher Sr and lower Nd and Pb isotope ratios (Fig. 4). The mafic ($Mg\# > 62$ where $Mg\# \equiv 100\ Mg/(Mg+Fe)$), low-$SiO_2$ (<44 wt%) lavas from the eastern Canary Islands have isotope compositions similar to those of the western Canary Islands and the LVC. Lavas with higher SiO_2 (>44 wt%) and/or lower Mg# (<62) have less radiogenic Pb and more radiogenic Sr than the LVC. Correlations between the degree of differentiation and isotope ratios indicate a shallow origin for the component with unradiogenic Pb, presumably located within the lithosphere[19,6].

Mafic volcanic rocks from central Europe show continuous, negative trends for Sr versus Nd and Pb versus Sr, and a positive trend for Pb versus Nd (Fig. 4*b*, *c*). As $^{206}Pb/^{204}Pb$ decreases, these data approach the compositions of deep-sea sediments on the Pb–Pb isotope diagram (Fig. 4*a*). The arrays for these mafic volcanic rocks are generally consistent with mixing between two components[18]. Component A, which has major- and trace-element characteristics of melilite nephelinite and isotope characteristics of the LVC, is interpreted as having a sublithospheric origin[18,22]. Component B has $^{87}Sr/^{86}Sr \cong 0.705$, $^{143}Nd/^{144}Nd = 0.5125$, and lies above the Northern Hemisphere reference line (NHRL) at $^{206}Pb/^{204}Pb \cong 18.0$. It has trace element and isotope compositions similar to granulite and hydrous spinel peridotite xenoliths entrained within the magmas, and probably has a lithospheric origin[18,23].

Volcanic rocks from the western Mediterranean domain define curvilinear Pb–Sr and Pb–Nd isotope arrays (Fig. 4). These volcanic rocks can be divided into two groups based on isotope composition and tectonic setting. Sodic ($Na_2O/K_2O > 0.7$) lavas from Mt Etna, Sicily[24–26], Straits of Sicily[27] and Pietre Nere, southeastern Italy[28] have Sr- Nd- and Pb-isotope ratios that overlap the LVC. Potassic and calc-alkaline lavas from regions influenced by recent subduction of the African plate (western Italy and the Aeolian Islands) extend to very high $^{87}Sr/^{86}Sr$ and to low $^{143}Nd/^{143}Nd$ and $^{206}Pb/^{204}Pb$ ratios. Lavas from western Italy have the most extreme isotope compositions, with values similar to deep-sea sediments (Fig. 4*a*), whereas lavas from the Aeolian Islands fall in the middle of the array. Oxygen-isotope data and positive europium anomalies in samples from western Italy provide additional evidence that the contamination involves a sedimentary component, probably subducted to shallow depths in the upper mantle[29,30] and located within the upper crust[59]. Minor amounts of a third, MORB-like component are also seen in some lavas from the Aeolian Islands[31], and in ancient tholeiites from Mt Etna[24,26].

The isotope data for the regions situated above the LVA (the eastern Atlantic, central Europe and the western Mediterranean) all converge to a narrow compositional range. This low-velocity composition (LVC; see earlier) has $^{87}Sr/^{86}Sr \cong 0.7030–0.7034$, $^{143}Nd/^{144}Nd \cong 0.51282–0.51294$ ($\varepsilon_{Nd} = 3.5–5.9$), $^{206}Pb/^{204}Pb \cong 19.9–20.1$, $^{207}Pb/^{204}Pb \cong 15.62–15.68$, $^{208}Pb/^{204}Pb \cong 39.60–39.90$, and is interpreted to represent a sublithospheric mantle source beneath each geographical region. The LVC is readily distinguished from the mantle source for N-MORB, in that it has relatively radiogenic $^{206}Pb/^{204}Pb$ and $^{87}Sr/^{86}Sr$, and lower $^{143}Nd/^{144}Nd$ compared to most MORB. Hotspot volcanism in the regions surrounding the LVA, such as the Ahaggar, Cameroon Line, Azores, Iceland and the Cape Verde Islands, have compositions which are similar to some of the volcanic rocks above the LVA, but none of the isotope trends for these hotspots converge precisely on an endmember with the composition of the LVC.

As noted from the tomography, an important question concerns the structure of the LVA. Does it represent one large upwelling region or multiple smaller, discrete upwellings? Evidence for the presence of the LVC is found in all tectonic environments above the LVA, including: (1) regions associated with rifting and extension, such as the NNE rift belt running through central Europe (including the Massif Central, the Rhenish massif and the Rhine graben), the Eger graben, and the straits of Sicily; (2) regions associated with subduction, such as western Italy and the Aeolian Islands; (3) back-arc basins, such as the Pannonian basin; (4) hotspots, such as the Canary Islands, Madeira Islands and possibly Mt Etna. The ubiquitous presence of the LVC over such a large region irrespective of tectonic regime is a potent argument that the LVA represents a common mantle source reservoir with a distinguishable isotope composition. The fact that this isotope composition is relatively uniform, and distinct from the mantle source for MORB, also suggests a deep origin from a well mixed reservoir. The combined evidence from seismic tomography and isotope geochemistry is therefore consistent with the interpretation that the LVA is a common source reservoir for the least-contaminated volcanic rocks found in the region extending from the eastern Atlantic to central Europe and the western Mediterranean.

Regional tectonics and distribution of volcanism

A long-standing problem in the regional tectonics of Europe has been how to explain the opening of the western Mediterranean basin through extension, rifting and sea-floor spreading, even though the African/European plate boundary has been undergoing compression during the Eocene and early Miocene[32]. This problem is well illustrated by the southward rifting of the Sardinia–Corsica ridge and the Balearic ridge away from France and

Spain, respectively, at the same time that Africa was colliding from the south. We find that the slowest seismic velocities, and presumably the hottest mantle material, are located beneath the Gulf of Valencia and the North Balearic basin, which separate the Sardinia–Corsica ridge and the Balearic ridge from the mainland. This correlation suggests a causal relationship between the extension and underlying thermal anomaly.

Volcanism is typically absent in continental regions undergoing compression and crustal and lithospheric thickening, such as in the Atlas Mountains, the Alps, the Pyrenees and along most of the Iberian peninsula, but is common in areas of crustal extension. The most voluminous volcanism in Europe is associated with the central European rift system, which extends NNE from the western Mediterranean to northwest Germany. Although poorly understood, the origin of lithospheric thinning and rifting in central Europe must have been influenced in part by the late stages of the Alpine orogeny[18,33]. Uplift and alkaline magmatism (in addition to more limited tholeiitic magmatism) associated with this extension, however, are difficult to explain solely through lithospheric thinning and seem to require a thermal anomaly in the underlying asthenospheric mantle[18,34]. Indeed, elevated heat flow from the mantle beneath the central European rift belt has been proposed as the cause of subcrustal upwarping and rifting[33]. The seismic and geochemical observations presented here are consistent with this interpretation. The NNE extensional belt, extending some 2,000 km from northwest Germany to the Algerian rift[8], parallels the trend of the upwelling sheet observed in the seismic tomography, and also for the most part overlies the slowest part of the velocity anomaly in model RG5.5. This correlation raises the intriguing possibility that the extensional belt may be the surface manifestation of the intersection of the upwelling sheet with the base of the lithosphere, with the surface location being modified to some degree by the effects of the Alpine, Pyrenean and Atlas orogenies.

The Eastern Atlantic volcanic province has the most voluminous volcanism. There has been a long-standing debate as to whether or not the origin of the Canary Islands is related to tectonic structures, such as the South Atlas fault, or to a mantle hotspot[3]. Several observations suggest that the Canaries are related to an asthenospheric feature rather than a lithospheric one. These include the lack of geophysical evidence for large fractures beneath the Canary Islands[3]; the east–west age progression, in the direction of plate motion, observed in both the subaerial (>20 to 0 Myr) and submarine (>60 to 3–4 Myr) volcanic sequences[17]; and evidence[35] that the parental magmas on Gran Canaria are derived from depths greater than 100 km. The NNE trend of the Eastern Atlantic volcanic province, which parallels the trend of the extensional belt of central Europe and the western Mediterranean, and the location of this volcanic province above the deep roots of the upwelling sheet, provide strong evidence for a connection with the underlying asthenospheric mantle.

Origin of the LVA

In contrast to three-dimensional models of mantle convection which show downwelling in sheets and upwelling as columns[36], the LVA appears to be sheet-like in model RG5.5, striking to the NNE and dipping to the west. As discussed above, planar upwelling is consistent with the large-scale tectonic features, in particular the NNE-trending rift belt extending through central Europe and the western Mediterranean, and with the distribution of volcanism in the area above the LVA. The westward dip of the LVA may reflect a combination of eastward asthenospheric flow[17] and lithospheric drag[37]. The areal extent of this upwelling sheet along the base of the lithosphere (2,500 by 4,000 km) is about twice that estimated for plume heads in the mantle[34,38]. White and McKenzie[34] proposed that plumes consist of a narrow (150–200 km across) central column, and a wide (1,000–2,000 km diameter) mushroom-shaped head of anomalously hot mantle (100–200 °C above ambient). Large heads (800–1,200 km diameter) have been predicted[38,39] for starting plumes derived from the core–mantle boundary, which may flatten to about twice their original diameter as they approach the overlying lithospheric plates. These models, however, are based on thermal plumes fed by narrow cylindrical conduits and so are not directly applicable to the feature discussed here.

Volcanism in each of the volcanic provinces can be traced back to the early Tertiary/late Cretaceous[4,5,8,18], suggesting that the mantle upwelling feature may be relatively long-lived. Considering the possible age and large size of this upwelling region, an important question is why continental rifting in central Europe has not progressed further, and why volcanism has not been more widespread. One possible explanation is that the temperature anomaly of this feature is not as large as that associated with hotspots such as Hawaii, or those which have produced flood basalts.

Plume heads that produce flood basalts are believed to be derived from the core–mantle boundary. High $^3He/^4He$ ratios at hotspots such as Hawaii and Iceland are consistent with derivation of at least some upwelling material from the deeper mantle[40–42]. Volcanic rocks from Mt Etna and the Canary Islands, however, have relatively low $^3He/^4He$ ratios, with a range of 5.8–7.5 R_A (refs 26, 42, and D.G., K.H., J. Lupton and H-U. Schmincke, manuscript in preparation). Furthermore, volcanic fluids from Italy and Europe show no evidence for $^3He/^4He$ ratios above MORB values[44–46]. Therefore, either the low-velocity anomaly is exclusively an upper-mantle feature, or it has been disconnected from a deep source for a sufficiently long time that the $^3He/^4He$ has been lowered by radiogenic ingrowth.

Available evidence from seismic tomography for a lower-mantle origin is equivocal. Global models SH12/WM13 and RG5.5 show this upper-mantle low-velocity anomaly extending only to depths of approximately 600–700 km (near the base of the transition zone in the upper mantle). Several seismic models[11,47], however, show a large-scale, low-velocity feature in the lower mantle farther to the south. If the LVA is just an upper-mantle feature fed from the boundary layer between the upper and lower mantle, this could explain why more extensive volcanism in Europe and the Mediterranean is absent and why continental rifting is still in its incipient stage.

These observations bear on the relationships between surface geochemistry, mantle dynamics and plate tectonics. Models for mantle convection have generally assumed that hotspots are underlain by thermal anomalies with a cylindrical geometry, and that the scale of these upwelling regions is considerably smaller (200–400 km in diameter) than discussed here. Our study provides evidence for the existence of large, sheet-like upwellings which should be considered in models of volcanism, mantle convection and regional tectonics. □

Received 18 March 1994; accepted 26 January 1995.

1. Anderson, D. L., Tanimoto, T. & Zhang, Y.-s. *Science* **256,** 1601–1732 (1992).
2. Feraud, G. *et al. Bull. volcanol.* **44,** 359–375 (1981).
3. Schmincke, H.-U. in *Geology of the Northwest African Margin* (eds Rad, U.v., Hinz, K., Sarnthein, M. & Seibold, E.) 273–306 (Springer, New York, 1982).
4. Holik, J. S. & Rabinowitz, P. D. *J. geophys. Res.* **96,** 12039–12067 (1991).
5. Le Bas, M. J., Rex, D. C. & Stillman, C. J. *Geol. Mag.* **123,** 287–298 (1986).
6. Hoernle, K., Tilton, G. & Schmincke, H.-U. *Earth planet. Sci. Lett.* **106,** 44–63 (1991).
7. Wedepohl, K. H. *Contr. Miner. Petrol.* **89,** 122–143 (1985).
8. Dercourt, J. *et al. Tectonophysics* **123,** 241–315 (1986).
9. Zhang, Y.-S. thesis, California Inst. Technol. (1991).
10. Zhang, Y.-S. & Tanimoto, T. *Nature* **355,** 45–49 (1992).
11. Su, W.-J., Woodward, R. L. & Dziewonski, A. M. *J. geophys. Res.* **99,** 6945–6980 (1994).
12. Snieder, R. *J. geophys. Res.* **93,** 12067–12080 (1988).
13. Zielhuis, A. & Nolet, G. *Science* **265,** 79–81 (1994).
14. Zielhuis, A. & Nolet, G. *Geophys. J. Int.* **117,** 655–676 (1994).
15. Spakman, W. *Geophys. J. Int.* **107,** 309–332 (1991).
16. Spakman, W., Lee, S.v.d. & Hilst, R.v.d. *Phys. Earth planet. Inter.* **79,** 3–74 (1993).
17. Hoernle, K. & Schmincke, H.-U. *J. Petrol.* **34,** 599–626 (1993).
18. Wilson, M. & Downes, H. *J. Petrol.* **32,** 811–849 (1991).
19. Hoernle, K. A. & Tilton, G. R. *Schweiz. Miner. petrogr. Mitt.* **71,** 3–18 (1991).
20. Hoernle, K., Schmincke, H.-U. & Tilton, G. (abstr.) *Eos* **72,** 528 (1991).
21. Halliday, A. N. *et al. Nature* **359,** 623–627 (1992); *Nature* **362,** 184 (1993).
22. Blusztajn, J. & Hart, S. R. *Geochim. cosmochim. Acta* **53,** 2689–2696 (1989).
23. Embey-Isztin, A. *et al. J. Petrol.* **34,** 317–343 (1993).

24. Carter, S. R. & Civetta, L. *Earth planet. Sci. Lett.* **36,** 168–180 (1977).
25. Carter, S. R., Evensen, N. M., Hamilton, P. J. & O'Nions, R. K. *Earth planet. Sci. Lett.* **37,** 401–408 (1978).
26. Graham, D., Giacobbe, A., Spera, F. & Tilton, G. (abstr.) *Eos* **73,** 611 (1992).
27. Mahood, G. A., Halliday, A. N. & Hildreth, W. *IAVCEI Abstr. Vol.* (IAVCEI, Mainz, 1990).
28. Vollmer, R. *Geochim. cosmochim. Acta* **40,** 283–295 (1976).
29. Rogers, N. W., Hawkesworth, C. J., Parker, R. J. & Marsh, J. S. *Contr. Miner. Petrol.* **90,** 244–257 (1985).
30. Rogers, N. W., Hawkesworth, C. J., Mattey, D. P. & Harmon, R. S. *Geology* **15,** 451–453 (1987).
31. Ellam, R. M., Hawkesworth, C. J., Menzies, M. A. & Rogers, N. W. *J. geophys. Res.* **94,** 4589–4601 (1989).
32. Dewey, J. F., Helman, M. L., Turco, E., Hutton, D. H. W. & Knott, S. D. *Kinematics of the Western Mediterranean* 265–283 (Spec. Publ. No. 45, Geol. Soc., Blackwell Scientific, Boston, 1989).
33. Illies, J. H. *Tectonophysics* **73,** 249–266 (1981).
34. White, R. S. & McKenzie, D. J. *geophys. Res.* **94,** 7685–7729 (1989).
35. Hoernle, K. & Schmincke, H.-U. *J. Petrol.* **34,** 573–597 (1993).
36. Bercovici, D., Schubert, G. & Glatzmaier, G. A. *Science* **244,** 950–955 (1989).
37. Griffiths, R. W. & Campbell, I. H. *Earth planet. Sci. Lett.* **103,** 214–227 (1991).
38. Griffiths, R. W. & Campbell, I. H. *Earth planet. Sci. Lett.* **99,** 66–78 (1990).
39. Campbell, I. H. & Griffiths, R. W. *Earth planet. Sci. Lett.* **99,** 79–93 (1990).
40. O'Nions, R. K. & Oxburgh, E. R. *Nature* **306,** 429–431 (1983).
41. Allègre, C. J., Staudacher, T., Sarda, P. & Kurz, M. *Nature* **303,** 762–766 (1983).
42. Kellogg, L. H. & Wasserburg, G. J. *Earth planet. Sci. Lett.* **99,** 276–289 (1990).
43. Vance, D. J., Stone, J. O. H. & O'Nions, R. K. *Earth planet. Sci. Lett.* **96,** 147–160 (1989).
44. Greisshaber, E., O'Nions, R. K. & Oxburgh, E. R. *Chem. Geol.* **99,** 213–235 (1992).
45. Hooker, P. J., O'Nions, R. K. & Oxburgh, E. R. *Nature* **318,** 273–275 (1985).
46. Matthews, A., Fouillac, C., Hill, R., O'Nions, R. K. & Oxburgh, E. R. *Earth planet. Sci. Lett.* **85,** 117–128 (1987).
47. Fukao, Y., Maruyama, S., Obayashi, M. & Inoue, H. *J. geol. Soc. Jap.* **100,** 4–23 (1994).
48. Skilbeck, J. N. & Whitehead, J. A. *Nature* **272,** 499–501 (1978).
49. Hart, S. R. *Nature* **309,** 753–757 (1984).
50. Sun, S.-S. *Phil. Trans. R. Soc.* A**297,** 409–455 (1980).
51. Ben Othman, D., White, W. M. & Patchett, J. *Earth planet. Sci. Lett.* **94,** 1–21 (1989).
52. Cousens, B. L., Spera, F. J. & Tilton, G. R. *Earth planet. Sci. Lett.* **96,** 319–335 (1990).
53. Wörner, G., Zindler, A., Staudigel, H. & Schmincke, H.-U. *Earth planet. Sci. Lett.* **79,** 107–119 (1986).
54. Nelson, D. R., Chivas, A. R., Chapell, B. W. & McCulloch, M. T. *Geochim. cosmochim. Acta* **52,** 1–17 (1987).
55. Francalanci, L., Taylor, S. R., McCulloch, M. T. & Woodhead, J. D. *Contr. Miner. Petrol.* **113,** 300–313 (1993).
56. Esperanca, S., Crisci, G. M., Rosa, R. D. & Mazzuoli, R. *Contr. Miner. Petrol.* **112,** 450–462 (1992).
57. Hawkesworth, C. J. & Vollmer, R. *Contr. Miner. Petrol.* **69,** 151–169 (1979).
58. Saltars, V. J. M., Hart, S. R. & Panto, G. *Mem. Am. Ass. Petrol. Geol.* **45,** 279–292 (1988).
59. Ferrara, G., Preite-Martinez, M., Taylor, H. P. Jr, Tonarini, S. & Turi, B. *Contr. Miner. Petrol.* **92,** 269–280 (1986).

ACKNOWLEDGEMENTS. We especially thank G. R. Tilton, J. Gill and T. Lay for providing analytical and computational facilities, and M. Hort, J. Gill, C. Lundstrom and C. Dunlap for comments on the manuscript. G. Mahood and H.-U. Schmincke helped stimulate some of the ideas in this study by pointing out geochemical similarities between volcanic rocks from Gran Canaria and from Pantelleria and the Eifel, respectively. We also thank W. Su, W. Spakman, R. Snieder and A. Zielhuis for helpful discussions and for providing copies of their seismic models, and W. Spakman, K. Spencer and H. Downes for reviews. This work was supported by the US NSF.

LETTERS TO NATURE

Avalanche mixing of granular solids

Guy Metcalfe, Troy Shinbrot, J. J. McCarthy & Julio M. Ottino*

Department of Chemical Engineering, Northwestern University, Evanston, Illinois 60208–3120, USA

THE production of many goods, ranging from pharmaceuticals and foods to polymers and semiconductors, depends on reliable, uniform mixing of solids. Although there have been several notable recent advances[1–6], solid mixing processes are still poorly understood. We can neither qualitatively nor quantitively determine the effectiveness of any given mixing process in advance. In contrast to the case of liquid mixing[7], we do not have a widely accepted theoretical basis that describes the mixing of solids. Moreover, we cannot determine whether a given set of solids will mix or separate during a specified stirring process[8–23]. As a step towards uncovering the basic physical principles, it is helpful to analyse systems that are both experimentally and theoretically tractable. Here we describe a geometric technique for the analysis of slow granular mixing processes, as are commonly encountered in industry. By comparing our calculations with experiments on thin rotating containers partially filled with coloured particles, we demonstrate that the mixing behaviour of powders in slow flows can be divided into geometric and dynamic parts. For monodisperse, weakly cohesive particles, geometric aspects dominate.

As an example of a system to be modelled, consider an upright two-dimensional disk partially filled with coloured passive particles and rotating about its axis (Fig. 1). For slow rotation, the surface layer mixes through the action of successive avalanches. Slow mixing implies that each avalanche stops completely before a new one begins. The avalanche duration scales as $\sqrt{D/g}$, where D is the container diameter and g is the acceleration due to gravity, so we require $\Omega\sqrt{D/g} \ll 1$, where Ω is the rotation rate. Material below the surface layer rotates as a solid body with the disk.

Experimentally, the disk is thin enough for the dynamics to occur in a plane. We note that although individual grains in the experiment may take a three-dimensional path during an avalanche, we observe through the front and back of the glass disk that the macroscopic features—boundaries, streaks and so on—extend entirely through the material layer, and consequently large-scale structures remain planar and the experimental flow may be assumed to be two-dimensional. The particles used are dyed table-salt grains—cubes with a mean side length of 0.6 mm—and the disk is 240 grains in diameter and 40 grains deep. An avalanche occurs when the surface slope exceeds $\theta_i \approx 60°$, after which the surface returns to its angle of repose, $\theta_f \approx 52°$, as sketched in Fig. 1; for salt we measure $\theta_i - \theta_f = 8° \pm 2°$.

The detailed mechanism for avalanches is not entirely understood and has been the topic of considerable research[1–6,24,25]. However, these details are not important here. The crucial point is that the surface motion that causes mixing is iterative; that is, one avalanche looks much like another, and the process of mixing can be represented as successive, nearly identical, avalanches which are repeated over and over.

The idea of the model is as follows. Consider any closed and slowly rotating mixing vessel, partially filled with granular material. Industrial examples of this kind of mixer include the V-blender[3], the tube or drum mixer, and the rotating kiln. The crucial observation is that irrespective of the detailed dynamics of the avalanche itself, the result of the avalanche is to transport an initial wedge of material (dark grey in Fig. 1) downhill to a new wedge (white in Fig. 1). Thus we can divide the problem of avalanche mixing into two distinct parts: transport *of* wedges and transport *within* wedges. The transport of wedges is geometrical and the transport within wedges can be represented mathematically by a map. As we will show, even without knowing the details of the dynamics within the wedges, it is possible to predict the mixing behaviour to a surprising degree of accuracy.

Consider now the special case of the disk shown in Fig. 1. Transport between wedges occurs only in areas where successive wedges intersect. These intersections take the shape of quadrilaterals whose size varies with fill level, f, defined as the fraction of the diameter occupied by the grains. For uniformly convex containers, analysis immediately reveals the following. (1) For $f < 0.5$, the quadrilateral intersections widen as the fill level

* To whom correspondence should be addressed.